AIP | Review of Scientific Instruments

Comparison between off-resonance and electron Bernstein waves heating regime in a microwave discharge ion source

G. Castro, D. Mascali, F. P. Romano, L. Celona, S. Gammino et al.

Citation: Rev. Sci. Instrum. **83**, 02B501 (2012); doi: 10.1063/1.3662477
View online: http://dx.doi.org/10.1063/1.3662477
View Table of Contents: http://rsi.aip.org/resource/1/RSINAK/v83/i2
Published by the American Institute of Physics.

Comparison between off-resonance and electron Bernstein waves heating regime in a microwave discharge ion source[a)]

G. Castro,[1,2,b)] D. Mascali,[1,3] F. P. Romano,[1,4] L. Celona,[1] S. Gammino,[1] D. Lanaia,[1] R. Di Giugno,[1,2] R. Miracoli,[1,2] T. Serafino,[3] F. Di Bartolo,[5] N. Gambino,[1,2,6] and G. Ciavola[1]

[1]*INFN- Laboratori Nazionali del Sud, via S. Sofia 62, 95123 Catania, Italy*
[2]*Università degli Studi di Catania, Dipartimento di Fisica e Astronomia, V. S. Sofia 64, 95123 Catania, Italy*
[3]*CSFNSM, Viale A. Doria 6, 95125 Catania, Italy*
[4]*CNR-IBAM Via Biblioteca 4, 95124 Catania, Italy*
[5]*Università di Messina, Ctr. da Papardo-Sperone, 98100 Messina, Italy*
[6]*IET-Institute of Energy Technology, LEC-Laboratory for Energy Conversion, ETH Zurich, Sonneggstrasse 3, CH-8092 Zurich, Switzerland*

(Presented 14 September 2011; received 12 September 2011; accepted 4 October 2011; published online 6 February 2012)

A microwave discharge ion source (MDIS) operating at the Laboratori Nazionali del Sud of INFN, Catania has been used to compare the traditional electron cyclotron resonance (ECR) heating with an innovative mechanisms of plasma ignition based on the electrostatic Bernstein waves (EBW). EBW are obtained via the inner plasma electromagnetic-to-electrostatic wave conversion and they are absorbed by the plasma at cyclotron resonance harmonics. The heating of plasma by means of EBW at particular frequencies enabled us to reach densities much larger than the cutoff ones. Evidences of EBW generation and absorption together with X-ray emissions due to high energy electrons will be shown. A characterization of the discharge heating process in MDISs as a generalization of the ECR heating mechanism by means of ray tracing will be shown in order to highlight the fundamental physical differences between ECR and EBW heating. © *2012 American Institute of Physics*. [doi:10.1063/1.3662477]

I. THEORETICAL BACKGROUND

Microwave discharge ion sources (MDISs) are used to produce high intensity proton beams (above 30 mA) with low emittance (below 0.2 πmm mrad). The operations of these devices are essentially based on the so-called off-resonance discharge in a quasi-constant magnetic field $B \sim 0.1$ T, obtained by launching electromagnetic (EM) waves with $f = 2.45$ GHz inside a metallic cavity of few cm of length and diameter.[1,2] Such devices are density limited, if the ECR is the only heating mechanism: the electromagnetic waves cannot propagate over a certain density, called cutoff density.[3] In such a way, one can obtain plasmas with densities only slightly above the O mode cutoff. The plasma density is a crucial parameter for the source performances because the output proton current depends linearly on it. To overcome the density limitations, electrostatic Bernstein waves (EBW) heating[4] is an option. Electrostatic waves, and in particular the EBW, do not suffer any density cutoff; they are able to propagate in largely overdense plasmas, i.e., plasmas above the cutoff, being absorbed at cyclotron harmonics.[5] EBW cannot propagate outside the plasma and they are internally created from an EM wave. It can be shown that X waves convert into EBW and ion waves at upper hybrid resonance (UHR),[6,7] when $\omega_{RF} = \sqrt{\omega_p^2 + \omega_c^2}$, ω_p being the plasma frequency and ω_c the cyclotronic frequency. The absorption mechanism can be explained by the Segdeev-Shapiro damping model, which predicts the creation of shell-like energetic electron layers where EBW are absorbed. According to Ref. 8, the wave energy can be absorbed by the electrons as in the case of Landau damping for longitudinal and magnetic field parallel waves. Because of the external B field, an $\vec{E} \times \vec{B}$ drift can arise. In a cylindrical symmetry, this drift forms an azimuthal flow rotating around the plasma axis. Viscosity and nonlinear phenomena could then generate a 3D, "typhoon-shaped" plasma vortex.[9]

II. EXPERIMENTAL SETUP

During the experiment, two different microwave discharge ion sources have been used, featuring slightly different magnetic profiles. The first one is a plasma reactor consisting of a stainless-steel cylinder 24 cm long, 14 cm diameter. A NdFeB permanent magnets system generates an off-resonance magnetic field along the plasma chamber axis (with a maximum of 0.1 T on axis). The second is the versatile ion source[10,11] (VIS). The source body consists of a water-cooled copper plasma chamber (100 mm long and 90 mm diameter). VIS enables us to have purely off-resonance microwave injection (which is not possible using plasma reactor). Microwaves have been generated by using a conventional 300 W magnetron, able to generate 2.45 GHz

[a)]Contributed paper, published as part of the Proceedings of the 14th International Conference on Ion Sources, Giardini Naxos, Italy, September 2011.

[b)]Author to whom correspondence should be addressed. Electronic mail: castrog@lns.infn.it.

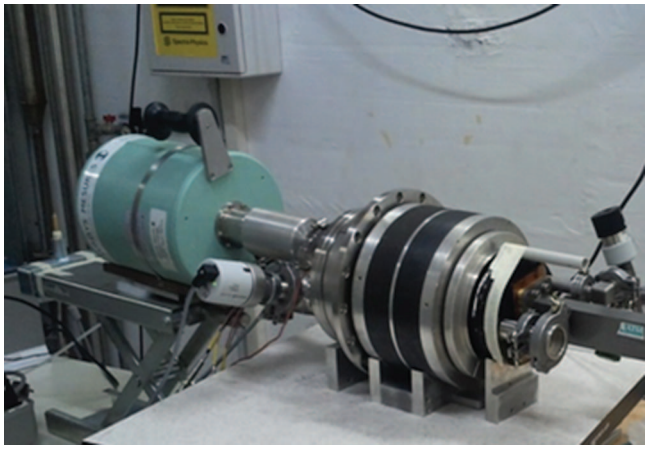

FIG. 1. (Color online) Render view of the experimental setup.

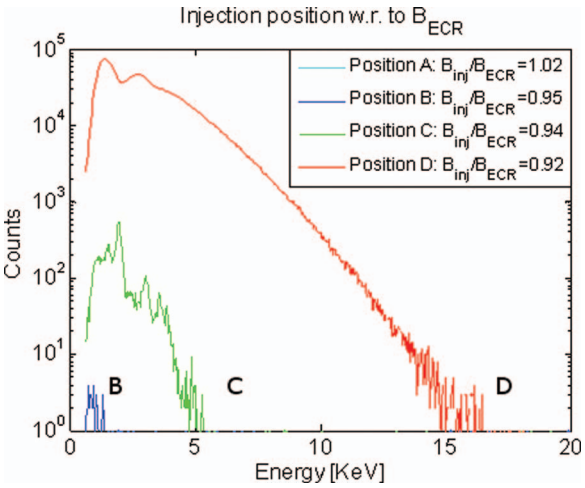

FIG. 3. (Color online) X ray detected at different positions of magnetic field. At position A, no X rays have been detected.

microwaves, or a travelling wave tube (TWT), able the generate microwaves from 3.2 to 4.9 GHz. The typical working frequency when using TWT was 3.7478 GHz. The measurements of temperature and plasma density have been carried out by using a movable Langmuir probe (LP). LP can host a small wire used as local electromagnetic antenna, which can be connected to a spectrum analyzer for the plasma spectral emission analysis. A Si-Pin and a HPGe X-ray detector have been used for the measurement of X-ray spectra in different plasma conditions. Both detectors are able to detect X rays with energy greater than about 1 keV. A CCD camera has been used to visualize the plasma structure within the chamber at the two working frequencies, at different microwave powers and pressures. A render view of the experimental set-up is shown in Figure 1.

III. EXPERIMENTAL RESULTS

In the first part of the experiment, we modified the position of the magnetic field with respect to the plasma chamber of VIS; in such a way, microwave injection takes place at different values of magnetic field. In each chosen configuration (see Figure 2), a measurement of X-ray emission has been done by means of Si-Pin X detector. In Figure 3, the results are shown. We use as reference B_{ECR}. X rays were detected particularly in position D ($B_{\mathrm{inj}}/B_{\mathrm{ECR}} = 0.92$, 1 keV spectral temperature). When the injection approaches B_{ECR}, X rays tend to disappear and finally, at position A ($B_{\mathrm{inj}}/B_{\mathrm{ECR}} > 1$), no X rays were detected. These results show that the production of high energy X rays (T > 1 keV) takes place only in case of under-resonance discharge, that is the required condition to have UHR placed somewhere inside the plasma. For $B_{\mathrm{inj}}/B_{\mathrm{ECR}} < 0.95$, the UHR takes place at quite high plasma densities, thus sustaining the production of a large number of warm electrons. Furthermore, the emittance measurements carried out in configurations A and D have shown a larger emittance in configuration D (0.207 π mm mrad) than in configuration A (only 0.125 π mm mrad). The emittance ε depends on the magnetic field at extraction B_{ext}, the radius of extraction r, the ratio of ion mass in amu to charge state of the

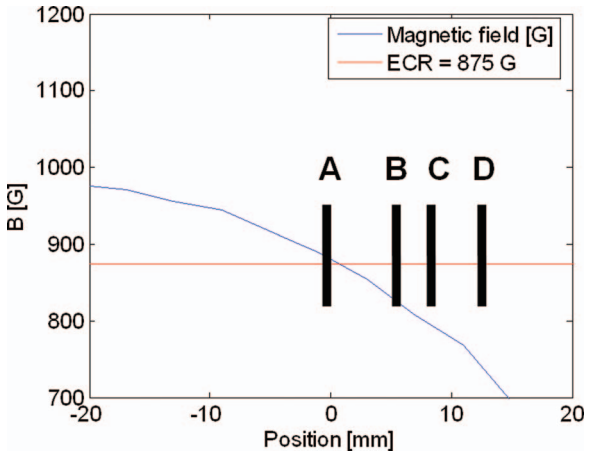

FIG. 2. (Color online) Position of Microwave injection with respect to the magnetic field. In configuration A, the injection occurs off-resonance; in configuration B, C, and D, the injection occurs under-resonance.

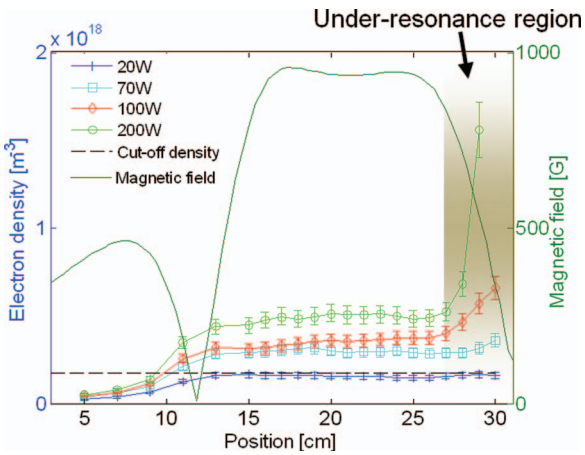

FIG. 4. (Color online) Electron density and magnetic field profile at 1.5×10^{-4} mbars, 2.45 GHz frequency at different microwave powers. Microwave injection occurs at the right-hand side of the figure.

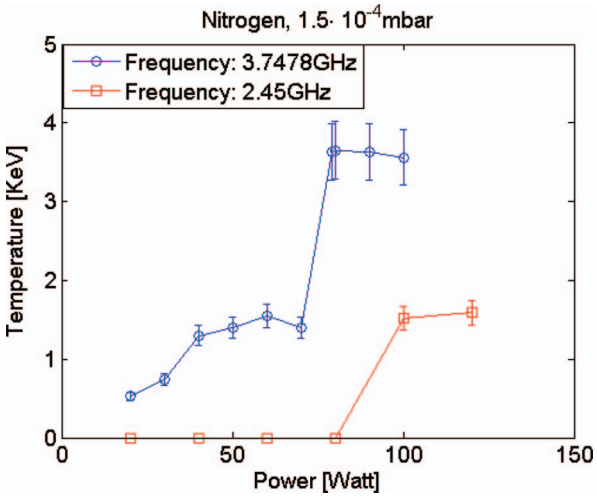

FIG. 5. (Color online) Spectral temperatures. At frequency of 2.45 GHz, ECR heating and EBW heating coexist; at 3.7478 GHz, EBW heating is dominant.

ion beam M/Q, and the root square of ionic temperature:[12,13]

$$\varepsilon = 0.016r\sqrt{\frac{kT_i}{M/Q}} + 0.032r^2 B_{\text{ext}}\frac{1}{M/Q}. \quad (1)$$

Since B_{ext} does not change significantly between configuration A and D, and r and M/Q are constant, it is probable that the production of ion waves at UHR causes strong ion heating, with a remarkable impact on beam emittance. In order to clarify the effects of EBW on electron density and temperature within the plasma chamber, a series of LP measurements has been carried out with the plasma reactor at the frequency of 2.45 GHz, when both under-resonance and off-resonance regions are present. In Figure 4, it is evident that the electron density is drastically enhanced in regions where condition $B < B_{\text{ECR}}$ is satisfied. This effect is observed for all different power values we used; in particular, at 200 W an electron density of about 1.5×10^{12} cm^{-3} has been measured, value twenty times greater than the cutoff density. Note that electron density is everywhere comparable or larger than the cutoff density ($n_c = 7.5 \times 10^{10}$ cm^{-3}). Analysis of probe data based on different probe theories confirmed these extremely high values. Plasma bulk temperature, on the contrary, does not change in the two regions. Higher values (about 14 eV) are present in proximity of ECR.

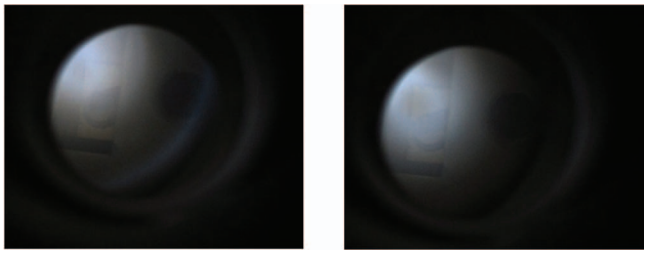

FIG. 6. Images of the plasma at $f = 2.45$ GHz and pressure $= 1.5 \times 10^{-4}$ mbars (on the left Microwave power is 20 W; on the right, it is 250 W).

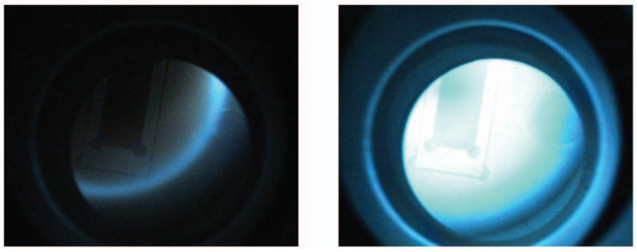

FIG. 7. (Color online) Images of the plasma at $f = 3.7478$ GHz and Pressure $= 1.5 \times 10^{-4}$ mbars (on the left Microwave power is 20 W; on the right, it is 250 W).

In the same magnetic configuration, X-ray measurements have been carried out at 2.45 GHz and 3.7478 GHz. By increasing the pumping frequency, it is possible to totally remove the ECR, so at 3.7478 GHz the entire plasma chamber is under-resonance and EBW heating becomes the unique heating mechanism. Spectral temperatures measured in the two cases are shown in Figure 5. At the frequency of 3.7478 GHz, the spectral temperature is significantly larger (up to 4 keV) rather than at 2.45 GHz. It is possible to identify, around 80 W, a threshold for which the slope of temperature increases suddenly and becomes steeper for both the configurations. End point energy is about ten times the value of the spectral temperature. The spectral temperature decreases slightly with the atomic mass of the used gas and when the pressure is increased.

An interesting correlation exists between the increase of the spectral temperature and CCD photos of the plasma. At low power, in both configurations a ring is visible, which disappears for $P > 80$ W. At 2.45 GHz, a plasma "ball" (probably due to direct ECR heating) is always present in the center of the chamber (see Figure 6). At 3.7478 GHz, as soon as the lateral ring disappears at higher power, the plasma assumes the structure of a plasma hole (Figure 7).[9] In both cases, the X-ray spectral temperature increases suddenly. It seems clear that the plasma goes through two metastable equilibrium configurations, each one characterized by a typical plasma shape and X-ray energy. A possible interpretation of these images is that the ring visible at lower power corresponds to UHR layer. By means of a ray tracing analysis (see Figure 8), it is possible to demonstrate that, if electron density decreases symmetrically from the chamber axis, going down below the cutoff value from the axis to the chamber walls, the UHR is placed laterally and it assumes a 3D structure very similar to the high brightness layers featured by the CCD images. In particular,

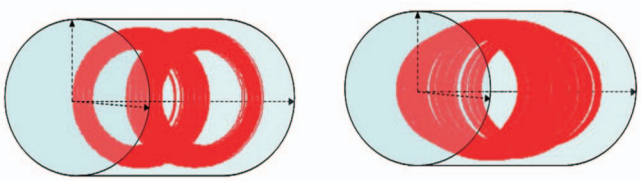

FIG. 8. (Color online) UHR position within the chamber calculated by means of ray tracing assuming an electron density decreases symmetrically from the chamber axis below the cutoff value (on the left $f = 2.45$ GHz, on the right $f = 3.7478$ GHz).

because of symmetry, UHR has the shape of two rings at 2.45 GHz, and of the lateral surface of a cylinder at 3.7478 GHz. When increasing the microwave power, the electron density in the peripheral regions increases accordingly, and the UHR cannot occur in this position. Plasma changes its shape and, in both cases, X-ray temperatures increase. In Ref. 14, it has been shown that hole at the center of the chamber represents a region at lower density. It is possible that in a plasma hole configuration UHR takes place in the central region of the chamber along the axis. Spatially resolved measurements along the radial direction will be needed to verify ray tracing predictions.

IV. COMMENTS

Measurements show that the presence of an under-resonance region in the injection side of the chamber enables us to reach densities up to twenty times the cutoff one by means of the absorption of EBW at cyclotronic harmonics. Generation of EBW with ancillary ion waves is confirmed by the enhancement of beam emittance, almost doubled. The increase of emittance is, however, much lower than the increase of electron density in the under-resonance region, thus finally producing a high brightness output beam. The measurements suggest that a source based only on EBW heating could reach very high density plasma (up to 1×10^{12} cm^{-3}) over the entire plasma chamber, and consequently extracted current much more intense than the ones obtained with typical devices used nowadays. Beams tools for reducing the emittance growth must be carefully investigated: gas mixing or passive "downstream" methods like space charge lens could be used to compensate the deterioration of beam quality in phase space caused by ion waves. Measurements show that the presence of UHR is accompanied by the presence of high energy X rays, which are created at cyclotronic harmonics when EBW are absorbed. X-ray spectral temperature and end point energy are strictly related to the plasma configuration. Hard plasma radiation is a clear sign of high energy electrons which can be used for multiple ionizations. Future high intensity multicharged ion sources can, therefore, be based on the results described here, by employing a simplified magnetic configuration with respect to typical B-minimum ECR ion sources.

ACKNOWLEDGMENTS

The support of the NTA-Helios Strategic Project of INFN and of the 5th National Committee is gratefully acknowledged. The authors are grateful to S. Tudisco, N. Gambino, L. Neri, G. Cosentino, A. Musumarra, and D. Santonocito for their support during experimental activity. The cooperation of L. Allegra and F. Chines has been essential for the present work. We acknowledge the financial support of the European Union Seventh Framework Programme FP7/2007-2013 under Grant Agreement No. 262010 – ENSAR. The EC is not liable for any use that can be made on the information contained herein.

[1] T. Taylor and J. S. C. Wills, Nucl. Instrum. Methods Phys. Res. A **309**, 37 (1991).
[2] G. Ciavola, S. Gammino, G. Raia, and J. Sura, Rev. Sci. Instrum. **65**, 1110 (1994).
[3] Y. Y. Podoba, H. P. Laqua, G. B. Warr, M. Schubert, M. Otte, S. Marsen, and F. Wagner, Phys. Rev. Lett. **98**, 255003 (2007).
[4] I. B. Bernstein, Phys. Rev. **109**, 10 (1958).
[5] K. S. Golovanivsky, V. D. Dougar-Jabon, and D. V. Reznikov, Phys. Rev. E **52**, 2969 (1995).
[6] H. P. Laqua, Plasma Phys. Control. Fusion **49**, R1 (2007).
[7] K. Budden, *The Propagation of Radio Waves* (Cambridge University Press, Cambridge, 1985), p. 596.
[8] R. Z. Sagdeev and B. D. Shapiro, Pis'ma Zh. Eksp. Teor. Fiz. **17**, 389 (1973).
[9] K. Nagaoka, A. Okamoto, S. Yoshimura, M. Kono, and M. Y. Tanaka, Phys. Rev. Lett. **89**, 075001 (1992).
[10] F. Maimone, G. Ciavola, L. Celona, S. Gammino, D. Mascali, N. Gambino, R. Miracoli, F. Chines, S. Passarello, G. Gallo, and E. Zappalà, "Status of the Versatile Ion Source VIS," *Proceedings of EPAC08*, Genoa, Italy, Vol. 868, p. MOPC151.
[11] R. Miracoli, L. Celona, G. Castro, D. Mascali, S. Gammino, R. Di Giugno, D. Lanaia, T. Serafino, and G. Ciavola, "Characterization of the Versatile Ion Source (VIS) and possible application as injector for future projects," Rev. Sci. Instrum. (these proceedings).
[12] I. G. Brown, *The Physics and Technology of Ion Sources* (Wiley, New York, 2004).
[13] M. P. Stockli, in *Proceedings of the 2001 Particle Accelerator Conference*, Chicago, IL, June 2001.
[14] D. Mascali, L. Celona, S. Gammino, R. Miracoli, G. Castro, N. Gambino, and G. Ciavola, Nucl. Instrum. Methods Phys. Res. A **653**, 11 (2011).